Integrative and Comparative Biology

Integrative and Comparative Biology, volume 59, number 2, pp. 420–431
doi:10.1093/icb/icz026

Society for Integrative and Comparative Biology

SYMPOSIUM

Bony Patchwork: Mosaic Patterns of Evolution in the Skull of Electric Fishes (Apteronotidae: Gymnotiformes)

Kory M. Evans,[1,*] Marta Vidal-García,[†] Victor A. Tagliacollo,[‡] Samuel J. Taylor[§] and Dante B. Fenolio[§]

*College of Food, Agricultural and Natural Resource Sciences, University of Minnesota, 1987 Upper Buford Circle, St. Paul, MN 55108, USA; [†]Research School of Biology, Department of Ecology and Evolution, The Australian National University, Canberra, ACT 0200, Australia; [‡]Museu de Zoologia da Universidade de São Paulo, Avenida Nazaré, 481, Ipiranga, 04263-000 São Paulo, Brazil; [§]Center for Conservation and Research, 3903 N. St Mary's Street, San Antonio, TX 78212, USA

From the symposium "Multifunctional structures and multistructural functions: Functional coupling and integration in the evolution of biomechanical systems" presented at the annual meeting of the Society for Integrative and Comparative Biology, January 3–7, 2019 at Tampa, Florida.

[1]E-mail: jacksonk@umn.edu

Synopsis Mosaic evolution refers to the pattern whereby different organismal traits exhibit differential rates of evolution typically due to reduced levels of trait covariation through deep time (i.e., modularity). These differences in rates can be attributed to variation in responses to selective pressures between individual traits. Differential responses to selective pressures also have the potential to facilitate functional specialization, allowing certain traits to track environmental stimuli more closely than others. The teleost skull is a multifunctional structure comprising a complex network of bones and thus an excellent system for which to study mosaic evolution. Here we construct an ultrametric phylogeny for a clade of Neotropical electric fishes (Apteronotidae: Gymnotiformes) and use three-dimensional geometric morphometrics to investigate patterns of mosaic evolution in the skull and jaws. We find strong support for a developmental, three-module hypothesis that consists of the face, braincase, and mandible, and we find that the mandible has evolved four times faster than its neighboring modules. We hypothesize that the functional specialization of the mandible in this group of fishes has allowed it to outpace the face and braincase and evolve in a more decoupled manner. We also hypothesize that this pattern of mosaicism may be widespread across other clades of teleost fishes.

Introduction

Mosaic evolution refers to the pattern where different traits of an organism experience different rates of evolution (Clarke and Middleton 2008; Felice and Goswami 2017). Here, organismal traits may elicit differential responses to selection or mutational pressures, unless constrained by conditioning on other traits (i.e., pleiotropy, integration) (Stebbins 1983; Cheverud 1996). Mosaic patterns of evolution can arise when semi-independent evolutionary modules (*sensu* Wagner 1996; Wagner and Altenberg 1996; Winther 2001), encompassing both functional and developmental components (Brandon 2005; Eble et al. 2005), elicit differential responses to selection, as a result of a low degree of covariation among modules and a high degree of covariation within modules (Felice and Goswami 2017).

The vertebrate skull is a multifunctional structure that has become a popular system for the study of modularity as several clades have evolved a diverse array of modular configurations (Goswami 2007; Drake and Klingenberg 2010; Goswami and Polly 2010; Sanger et al. 2012; Piras et al. 2014; Vidal-García and Keogh 2017). Teleost fishes in particular have evolved high kinetic skulls with protrusible jaws for use in suction feeding and have subsequently

Advance Access publication May 9, 2019

adapted their skulls to exploit a wide variety of trophic resources (Westneat 2004, 2005; Price et al. 2011). Trophic ecology is suspected to be a strong driver of morphological diversification in the skull of teleost fishes, as shifts to different feeding behaviors and prey items have been shown to exert differential selection pressures on feeding morphologies and performance (Wainwright et al. 1991, 2004; Westneat 2005; Helfman et al. 2009; Collar et al. 2014; Kolmann et al. 2018). Within the teleost skull, the mandible has become a widely used model for ecomorphological studies (Motta 1988; Wainwright et al. 1991; Liem 1993; Westneat 2005; Hill et al. 2018). The mandible has also been shown to exhibit high levels of developmental plasticity to environmental stimuli in members of several phylogenetically disparate teleosts clades, including cyprinids (Neuhauss et al. 1996; Trainor et al. 2003); salmonids (Küttner et al. 2014); centrarchids (Hegrenes 2001), and cichlids (Wimberger 1992; Chapman et al. 2008; Parsons et al. 2014; Hu and Albertson 2017).

Within teleost fishes, Neotropical electric fishes (Gymnotiformes: Teleostei) have become a popular system for the study of skull shape evolution and specifically, integration and modularity (Evans et al. 2017b, 2017c, 2018a; Keeffe et al. 2019). Gymnotiform fishes are a clade of elongate, weakly-electric fishes distributed in the freshwaters of Central and South America. This clade of fishes is particularly interesting for studies of skull shape evolution because they have evolved a remarkable diversity of skull shapes ranging from highly elongate faces (e.g., *Sternarchorhynchus*), to highly foreshortened faces (e.g., *Hypopygus*) with a wide range of intermediate phenotypes (Albert 2001; Evans et al. 2017b, 2018b). Previous studies looking at the neurocranium in two dimensions recovered strong patterns of evolutionary integration between the face and braincase across the entire clade and during the development of dolichocephalic (long-snouted) species (Evans et al. 2017b, 2017c). These patterns of strong evolutionary integration are thought to be driven by developmental mechanisms underlying the formation of the face. While informative, the previous studies were limited because they only examined two modules in the neurocranium, excluding the lower jaw (mandible) and associated elements and only examined these patterns of covariation in two dimensions, which may have excluded an important axis of shape variation in the third dimension (Buser et al. 2017). The exclusion of the lower jaw in previous literature limits insight into patterns of evolutionary integration across the entirety of gymnotiform skull. Unlike the neurocranium, the mandible is developmentally derived from a distinct neural crest cell (NCC) population, which eventually forms the Meckel's cartilage (Mabee and Trendler 1996). Within Gymnotiformes, the family Apteronotidae exhibit the highest degree of craniofacial shape diversity with phenotypes ranging from highly elongate tube-snouts (e.g., *Sternarchorhynchus*) to foreshortened faces (e.g., *Adontosternarchus*) with each phenotype accompanied by a unique trophic ecology that includes planktivory (e.g., *Adontosternarchus*) and lepidophagy (a specialized form of piscivory that consists of feeding exclusively on fish scales, e.g., *Sternarchella*) (Evans et al. 2017a).

Here, we examine patterns of evolutionary integration, modularity, and disparity in three dimensions across the skull of apteronotid fishes using geometric morphometrics and evaluate hypotheses of modularity across the teleost skull. We also quantify rates of shape evolution between modules to test for the presence of mosaic evolution across the apteronotid skull. We predict that the mandible will exhibit the highest degree of evolutionary modularity relative to the other hypothesized modules (face, orbit, and basicranium), due to its developmental semi-autonomy; as it is derived from a unique NCC population relative to aforementioned elements of the neurocranium; which are known to exhibit strong patterns of covariation early in development (Mabee and Trendler 1996; Marcucio et al. 2005; Parsons et al. 2018). We further predict that the mandible will exhibit the fastest rates of shape evolution as a result of its increased evolutionary modularity.

Materials and methods

Morphological sampling

Craniofacial shape was characterized across 49 species of apteronotid fishes (52% taxon sampling) representing 13 of 15 known genera (Supplementary Table S1). An average of 3.0 specimens per species were micro-CT scanned using a Bruker SkyScan 1172 at the University of Washington, in conjunction with the #ScanAllFishes project. Sampling was restricted to adult specimens (as evidenced by body size and degree of sphenoid ossification) to avoid potential biases introduced by ontogenetic shape differences (Evans et al. 2017b). Micro-CT scans were then used to construct surface models (.stl) of skulls for each specimen and imported into *Stratovan Checkpoint* © for digitizing. All three-dimensional models are freely available for download at Open

Science Framework (osf.io/q4aw5). Specimens were digitized in 3-dimensional with 25 landmarks placed on the left side of each specimen (Fig. 1) following Evans et al. (2018a) (Table 1).

Since one of the main questions of this study was to discern whether rates of shape evolution are different among modules in the head, we had to perform a single Procrustes analysis across all regions so that we would be able to compare evolutionary rates among them. However, this would entail using landmarks of both the skull and mandible, which would not only include their morphological variation, but also variation in the relative position of one structure to the other due to their articulated nature. We found variation in the relative position between the skull and jaws across all specimens (Supplementary Table S2), which would affect shape estimates as well as the quantification of integration between different cranial modules. In order to correct for this rotational variation across specimens, we performed a rigid rotation of all the mandible landmark subsets using the function *simple.rotation* in the ShapeRotator R tool (Vidal-García et al. 2018), in order to standardize the position of the skull and mandible relative to the jaw joint in the three-dimensional space across all specimens. This tool removes the effect of random translations and rotations across specimens, so that all regions are placed in homologous relative positions, allowing a single Generalized Procrustes Superimposition in a multimodular and articulated structure (Vidal-García et al. 2018).

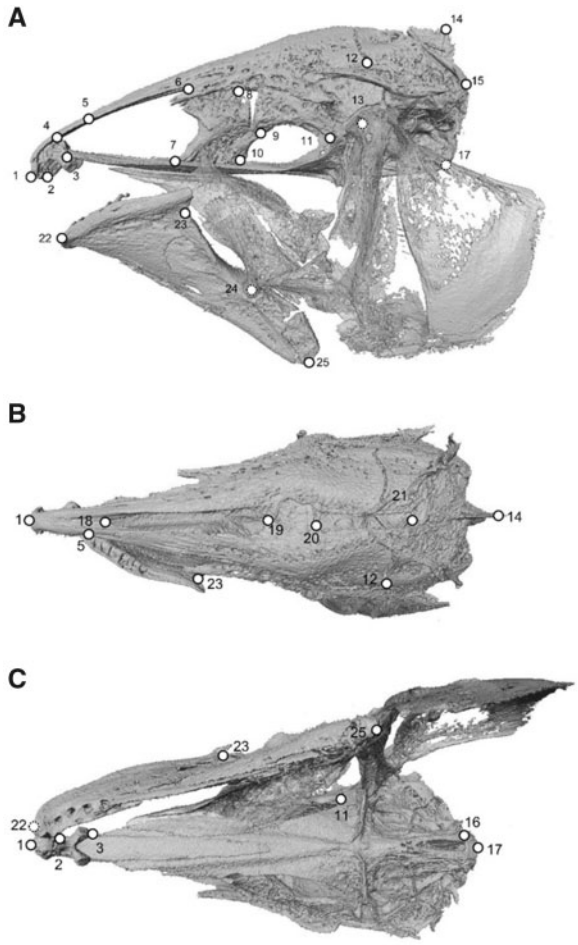

Fig. 1 CT scans of *Apteronotus bonapartii* in lateral (**A**), dorsal (**B**), and ventral (**C**) views showing 25 three-dimensional landmarks used for the geometric morphometric analysis of skull shape in apteronotid fishes.

Phylogenetic reconstruction

The package phylotaR (Bennett et al. 2018) was used to retrieve DNA sequences from GenBank release 230 (February 15 2019). This package is an updated version of the program PhyLoTa (Sanderson et al. 2008), which includes a pipeline that uses the Basic Local Alignment Search Tool—BLAST (Altschul et al. 1990) to identify and retrieve orthologous DNA sequences clusters. The pipeline consisted of four stages: taxise, download, cluster, and cluster2. The taxise stage identified taxonomic ranks of the clade Gymnotiformes (ID = NCBI:txid8002) available in the NCBI taxonomy database (Federhen 2012). The download stage hierarchically retrieved sequences from across all recognized taxonomic ranks. The cluster stage generated clusters from the downloaded sequences down to the taxonomic ranks. The cluster2 stage joined clusters identified within separate ranks to identify clusters at higher taxonomic ranks. Each cluster was exported as sequences in FASTA format and, then, aligned using MAFFT under default parameters (Katoh et al. 2005).

TrimAl: automated alignment trimming

The program trimAl (Capella-Gutiérrez et al. 2009) was used to automatically trim aligned sequences. This program adjusts models to optimize signal-to-noise ratios within alignments. It incorporates three basic algorithms for automated trimming alignments: gappyout, strict, and strictplus; each one of them applies a threshold of acceptable missing data (or gaps) and similarity scores (e.g., residue similarity scores—see the algorithm in Thompson et al. 2001). The option-automated was used in the program trimAl. This option implements a heuristic method using a decision tree approach to choose between either the algorithms gappyout or strict/strictplus depending on the features of the alignments. This option has been optimized for trimming

Table 1 Landmark descriptions and module hypotheses for the three-dimensional geometric morphometric analysis of skull shape

Landmark No.	Landmark description	Skull (no modules)	Skull and jaws	Face, braincase, and mandible	Ethmoid, orbit, basicranium, mandible
1	Mesethmoid-anterior-most tip	1	1	1	1
2	Mesethmoid-ventral ethmoid-mesethmoid ventral margin	1	1	1	1
3	Ventral ethmoid-ventral ethmoid-parasphenoid margin	1	1	1	1
4	Ventral ethmoid-ventral ethmoid-mesethmoid dorsal margin	1	1	1	1
5	Frontal-mesethmoid-frontal margin	1	1	1	1
6	Orbitosphenoid-anterior-most orbitosphenoid-frontal margin	1	1	1	2
7	Orbitosphenoid-anterior-most orbitosphenoid-parasphenoid margin	1	1	1	2
8	Pterosphenoid-orbitosphenoid-pterosphenoid-frontal margin	1	1	1	2
9	Pterosphenoid-orbitosphenoid-pterosphenoid ventral margin	1	1	1	2
10	Parasphenoid-posterior-most orbitosphenoid-parasphenoid margin	1	1	1	2
11	Parasphenoid-pterosphenoid-parasphenoid margin	1	1	2	2
12	Parietal-lateral-most parietal-frontal suture	1	1	2	3
13	Prootic–prootic foramen	1	1	2	3
14	Supraoccipital-posterior-most projection of supraoccipital crest	1	1	2	3
15	Supraoccipital-exoccipital-supraoccipital margin	1	1	2	3
16	Basioccipital-posterior-ventral-most point of basioccipital	1	1	2	3
17	Basioccipital-posterior-most-parasphenoid-basiocciptal margin	1	1	2	3
18	Frontal-anterior-most segment of anterior fontanel	1	1	1	2
19	Frontal-posterior-most segment of anterior fontanel	1	1	1	2
20	Frontal-anterior-most segment of posterior fontanel	1	1	2	2
21	Parietal-posterior-most segment of anterior fontanel	1	1	2	3
22	Dentary-anterior-most tooth	1	2	3	4
23	Dentary-dorsal-most-dentary-angular-margin	1	2	3	4
24	Angular-center of jaw joint	1	2	3	4
25	Retroarticular-posterior-ventral-most point on retroarticular	1	2	3	4

Module assignments denoted by Numbers 1–4 for different hypotheses.

alignments to be analyzed by maximum likelihood inferences (see manual at http://trimal.cgenomics.org/trimal).

PartitionFinder2: partitioning schemes and models of DNA evolution

The program PartitionFinder2 (Lanfear et al. 2016) was used to estimate simultaneously the optimal partitioning scheme and models of DNA evolution for the concatenated matrix. The model estimates were performed on a tree inferred by maximum parsimony and assuming linked branch lengths. When branch lengths are set to linked, the relative branch lengths are determined by the start tree, and each model is afforded a single rate multiplier which can stretch or shrink all branch lengths. Models of DNA evolution were restricted to either GTR or GTR + Γ. For large alignments, it is not practical to compute all possible models in PartitionFinder2. The relaxed hierarchical clustering algorithm (rclusterf) was used to compute and compare likelihoods across partitioning schemes. The best partitioning scheme was selected using the Akaike Information Criterion (AIC).

BEAST 2

The program BEAST 2 (Bouckaert et al. 2014) was used to estimate posterior trees of Gymnotiformes. Priors for substitution rates were taken from the output of PartitionFinder2. Priors for tree/branching were set to birth–death process. Priors for clock rates were set to an uncorrelated relaxed clock with log-normal distributions. Taxa with missing DNA sequences were randomly assigned within respective genera and/or families. BEAST ran two independent Markov Chain of Monte Carlo (MCMC) of 50

million generations each, sampling a tree topology and log parameters at every 5000 generations. The diagnosis of MCMC runs and posterior probabilities were evaluated by inspections of the effective sample sizes in the program Tracer (Rambaut and Drummond 2003). Burn-in procedure (25%) was defined after the inspection of the posteriors of the combined MCMC chains. Posterior trees were summarized in a maximum clade credibility (MCC) topology with node heights represented by median heights (Fig. 2). Besides the MCC topology, 100 random posterior trees were selected for conducting analyses of morphological evolution.

Integration and modularity

We fit four different models of craniofacial modularity to our dataset in order to identify the best modular partition using a phylogenetic adaptation of a maximum likelihood approach with the R package EMMLi (phyloEMMLi) (Goswami and Finarelli 2016) (Table 1; Supplementary Fig. S1). Our first model assumed no modularity across the skull. The second model consisted of two biomechanical functional modules (neurocranium and mandible) following the delimitations of Westneat (2005). Our third model consisted of three developmental modules (face, braincase, and mandible) following Langille and Hall (1988) and Evans et al. (2017b, 2017c). Our fourth model consisted of four modules (ethmoid, optic, basicranium, and mandible) based on the sensory capsules that serve as developmental precursors that form different regions of the neurocranium (excluding the otic region) and the developmentally distinct mandible (Helfman et al. 2009).

We also quantified the degree of phylogenetic integration for the four different modular partitions with the covariance ratio (CR) coefficient (Adams 2016) using the function *phylo.modularity* in geomorph (Adams 2016). We estimated the degree of modularity (CR), the bootstrapped 95% confidence intervals of the CR, and the *P*-values across the posterior distribution of 101 trees, in order to take into account phylogenetic uncertainty.

We then compared the phylogenetic mean rates of shape evolution among modules from the best supported modular partition hypothesis across all 101 trees.

Disparity through time

After recovering strong support for a three module hypothesis consisting of the face, braincase, and mandible regions, we used a disparity through time (DTT) analysis to examine patterns of shape evolution across the three modules separately. DTT analyses estimate the relative trait (in this case shape) disparity throughout time and compares the empirical data its pattern to an expected pattern under Brownian motion (BM). Recently, DTT approaches have been marred by issues related to multiple testing and high false-positive rates. In our analysis, we utilized a recent implementation of the DTT analysis which employs a rank envelope test that orders disparity curves based on their most extreme disparity values (for more information see Murrell 2018). All DTT analyses were performed using the r-package *geiger* (Harmon et al. 2008).

We ran separate DTT analyses for each of the three modules. Each module was subjected to a generalized Procrustes superimposition. DTT analyses

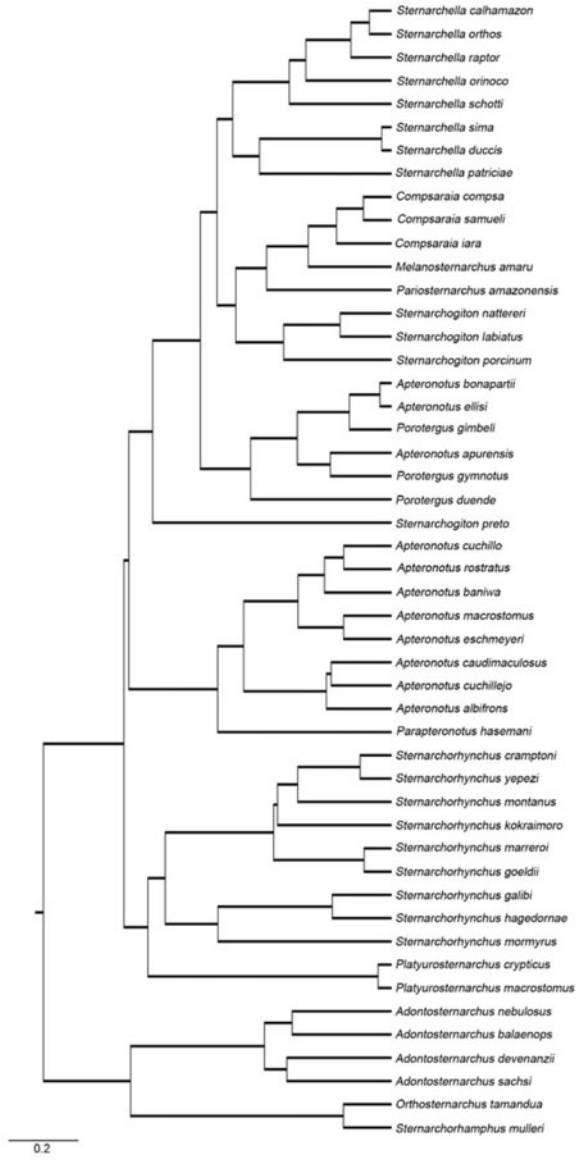

Fig. 2 MCC tree of 49 apteronotid species.

were then performed on the Procrustes coordinates of each module, each analysis consisted of 2500 simulations to construct the null BM disparity model. The null hypothesis (BM) was rejected whenever the DTT curve of a module was ranked in the 5% most extreme curves from the null model.

Results

Skull shape evolution in Apteronotidae

Apteronotid fishes exhibit a diverse array of skull shapes (Fig. 3). The primary axis of variation (PC1) explains 70.65% of the total shape variance and corresponds to shape differences in the neurocranium and dentary (anterior portion of the mandible). Along this axis, species range from exhibiting highly foreshortened neurocrania (truncated frontal and ethmoid regions) and dentaries (e.g., *Adontosternarchus balaenops*) to elongate neurocrania and dentaries, typical of the tube snouted species (e.g., *Sternarchorhynchus kokraimoro*). The second principal component axis (PC2) explains 11.10% of total shape variation and corresponds primarily to shape differences in the posterior portion of the mandible encompassing the jaw joint and retroarticular. Along this axis, species range from exhibiting truncated posterior regions of the mandible (e.g., *Orthosternarchus* and *Adontosternarchus*) to more elongate (e.g., *Apteronotus eschmeyeri*).

Evolutionary modularity

Analysis of evolutionary modularity using EMMLi indicates strong model support for a developmental three-module hypothesis encompassing the face, braincase, and mandible regions with different within and between-module ρ values (Table 2). A significant degree of modularity is also recovered using the CR with a median CR of 0.86 across the 101 randomly sampled phylogenies. Using the EMMLi analysis, we find that the mandible exhibits the highest degree of within-module correlation ($\rho = 0.79$) followed by the face ($\rho = 0.66$) and the braincase ($\rho = 0.46$). Additionally, we find that the face and mandible exhibit the highest degree of between-module correlation ($\rho = 0.62$) relative to the face and braincase ($\rho = 0.45$), and the braincase and mandible ($\rho = 0.42$).

In addition to differing levels of shape correlation among modules, we also recover significantly different rates of shape evolution between modules using the *compare.multi.evol.rates* analysis (Table 3 and Fig. 4). We find that the mandible evolves nearly four times (σ^2 ratio = 3.70) faster, on average, than either the face ($P < 0.001$) or braincase ($P < 0.001$) modules. Additionally, we find that the face and braincase evolve at indistinguishable ($P = 0.243$) rates.

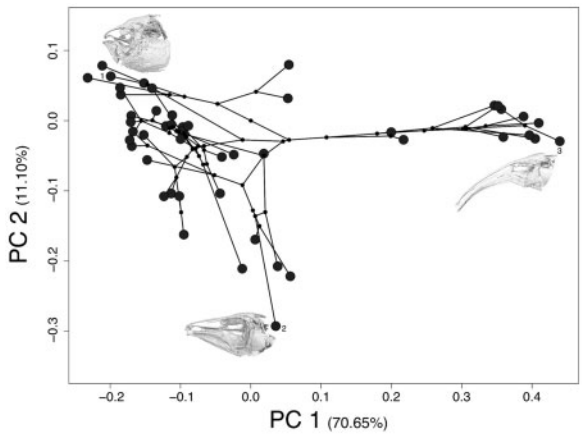

Fig. 3 Phylomorphospace analysis of skull shape for 49 apteronotid species showing the first two principal component axes. Insets depict extreme skull shapes for each axis. (1) *Adontosternarchus balaenops*, (2) *Apteronotus eschmeyeri*, and (3) *Sternarchorhynchus kokraimoro*.

Disparity through time

DTT analyses indicate differences in patterns of shape evolution between modules (Fig. 5). We find that both the face and mandible closely track a BM model of shape evolution (face: $P = 0.348$, MDI = 0.302) (mandible: $P = 0.318$, MDI = 0.254), while the braincase differs significantly ($P = <0.001$, MDI = 0) from a BM model and has maintained a fairly constant level of sub-clade disparity for much of its evolutionary history.

Discussion

Here we evaluated morphological disparity, modularity, and evolutionary integration in the skull and mandible of apteronotid fishes, using a three-dimensional geometric morphometric approach. We focused on the tempo and mode of morphological evolution in this clade by asking two main questions: (1) are patterns of shape evolution highly integrated across the head or do they instead follow a modular pattern? And (2) are there differential rates of shape evolution between modules in the skull (i.e., mosaic evolution)? We were able to identify a strongly supported tri-modular model consisting of the face, the braincase, and the mandible. We found that the mandible has evolved four times faster than the face and braincase. We hypothesize that the functional specialization and the developmental autonomy of the mandible in this group of fishes have resulted in higher rates of shape

Table 2 Results for the evaluation of modularity hypotheses (using EMMLI) for 49 apteronotid species

Model	*K*	AICc	ΔAICc	Model likelihood	Posterior probability
No modules	2	1088.88	333.56	3.70E−73	3.63E−73
Skull and mandible—same within-module p + same between-module p	3	1090.58	335.27	1.58E−73	1.55E−73
Skull and mandible—seperate within-module p + same between-module p	4	1029.28	273.97	3.23E−60	3.17E−60
Face, braincase jaws—same within-module p + same between-module p	3	991.88	236.57	4.27E−52	4.19E−52
Face, braincase, jaws—seperate within-module-p + same between-module p	5	862.65	107.34	4.92E−24	4.84E−24
Face, braincase jaws—one within-module p + seperate between-module ps	5	884.49	129.17	8.92E−29	8.77E−29
Face, braincase, jaws—seperate within-module-ps + seperate between-module ps	**7**	**755.31**	**0.00**	**1**	**0.98**
Ethmoid, orbit, basicranium, mandible—same within module p + same between module p	3	1064.16	308.85	8.60E−68	8.45E−68
Ethmoid, orbit, basicranium, mandible—seperate within module p + same between module p	6	926.95	171.63	5.38E−38	5.29E−38
Ethmoid, orbit, basicranium, mandible—same within module p + seperate between module p	8	900.41	145.10	3.10E−32	3.05E−32
Ethmoid, orbit, basicranium, mandible—seperate within module p + seperate between module p	11	763.41	8.10	0.02	0.02

Models correspond to modules in Supplementary Table S2, while additionally testing within and between module correlations (ρ). Bold text indicates optimal model.

evolution and a higher degree of modularity over evolutionary time. We discuss each of these topics in turn, and suggest that this pattern of morphological mosaicism is likely to be common throughout other clades of teleost fishes.

Mosaic evolution in the electric fish skull

Mosaic evolution occurs when different traits of an organism undergo differential rates of evolution. This is typically considered to be a product of the modularization of organismal traits, which subsequently allows them to elicit differential responses to selective pressures. Here, we find that the mandible evolves nearly four times faster than its neighboring modules; the face and braincase. Similarly, the mandible exhibits the highest degree of within module correlation relative to the other modules. These findings suggest that the mandible may exhibit a higher degree of autonomy than the face or braincase, and that this autonomy may have subsequently allowed the mandible to exhibit substantially faster rates of shape evolution. A potential explanation for this autonomy may be found in the developmental prominences that form the upper and lower jaws. During development in bony fishes, the elements of the neurocranium are derived from a mixture of cranial NCCs, mesoderm, and frontonasal ectoderm, while the mandible is derived from a unique population of cranial NCCs located in the first pharyngeal arch which later form the Meckel's cartilage (Langille and Hall 1988; Benjamin 1990). This cartilage eventually ossifies and becomes part of the lower jaw. The timing of the ossification between the neurocranium and the mandible also differs substantially with the Meckel's cartilage, typically appearing and ossifying earlier than many of the skeletal elements of the neurocranium (Mabee and Trendler 1996).

We hypothesize that the rates of shape evolution in the mandible are closely tracking the evolution of trophic ecology in Apteronotidae. Within Apteronotidae, species have evolved a broad diversity or trophic ecologies including planktivory (e.g., *Adontosternarchus*), lepidophagy (scale-eating; e.g., *Sternarchella raptor*), and a highly specialized form of invertivory involving grasp-suction feeding in several independently evolved tube-snouted species (e.g., *Orthosternarchus* and *Sternarchorhynchus*). The modularity of the mandible may allow it to exhibit a stronger response to trophic selective pressures as it is less constrained by conditioning (integration) on other regions of the skull. Interestingly, we find that

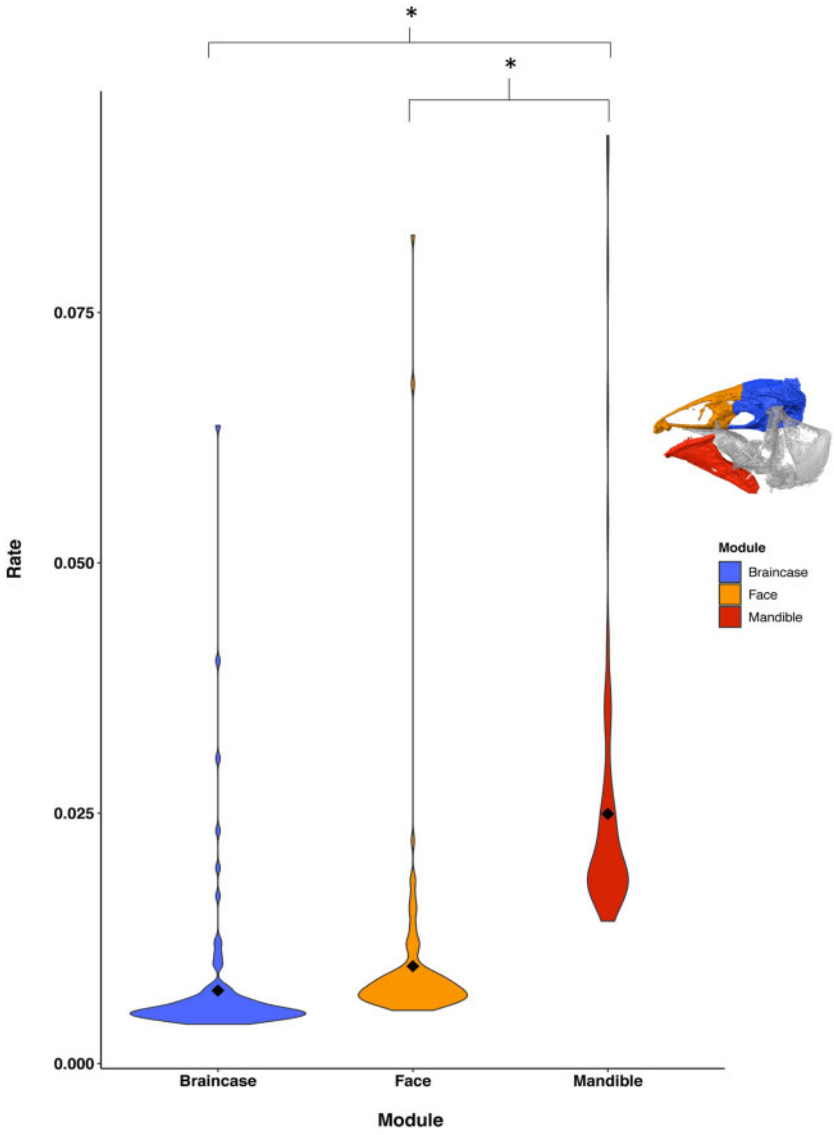

Fig. 4 Mosaic evolution in the apteronotid skull with violin plots depicting relative rates of shape evolution between modules across 101 phylogenies randomly sampled from a posterior distribution. Diamonds indicate mean rate values. Asterisks indicate statistical significance ($P = 0.05$). Inset depicts representative craniofacial regions.

Table 3 Results of the evolutionary modularity analysis showing rates of shape evolution (±standard error) averaged across 101 phylogenies sampled from a posterior distribution

Module	Rate (avg)	Std error
Face	0.0097	0.0010
Braincase	0.0073	0.0008
Mandible	0.0249	0.0014

the face and mandible exhibit the highest degree of between-module covariation, however, the mandible still evolved significantly faster than the face, while the face and braincase exhibited indistinguishable rates of shape evolution. The tight link between the mandible and the face is not surprising, given that the face typically houses the tooth-bearing premaxillary bones which function together with the mandible during prey capture and processing (i.e., functional integration). It is therefore possible that the face and mandible elicit similar directional responses to selective pressures, but that the face is constrained by its close proximity to the braincase and thus exhibits a lower degree of shape diversity across evolutionary time.

The highly conserved braincase

Under a neutral model of trait evolution, a strict correlation should generally exist between evolutionary rate and trait variance (Felsenstein 1985; Ricklefs 2006).

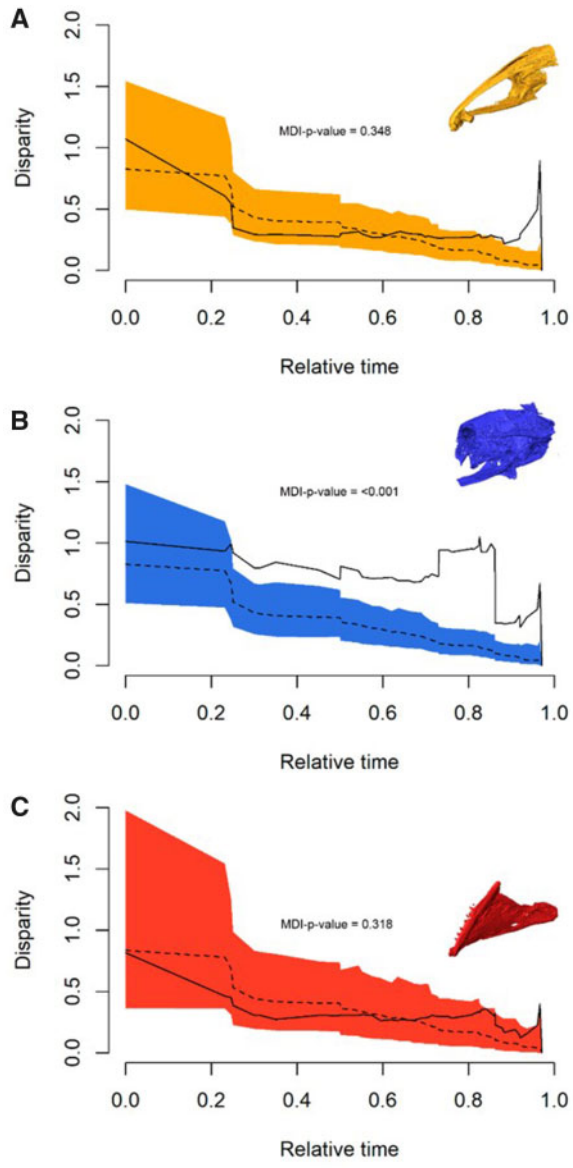

Fig. 5 DTT of the cranial modules in Apteronotidae. DTT analyses using the rank envelope test for face, braincase, and mandible modules showing the change in empirical (solid line) shape disparity over relative time when compared with a BM model (dashed line). Shaded areas indicate 95% confidence intervals. *P*-values reported are the most conservative from the results of the rank envelope test.

In other words, the relationship between disparity and rate should closely track a BM model of trait evolution (Felice et al. 2018). This is because under a BM model, trait variance is proportional to evolutionary rate. Deviations from the BM model are also possible depending on how selection acts on the underlying covariance structure of the traits and may be indicative of constraints or other forces that may have an influence on trait disparity. To test the relationship between disparity and relative time for the three craniofacial modules, we used a DTT analysis. We find that both the face and mandible follow a BM model of trait evolution while the braincase differed significantly from a BM process. The braincase appears to maintain a fairly constant level of disparity for over 80% of relative evolutionary time before steeply declining toward the recent, suggesting that the braincase is constrained in a way that prevents it from following the null model expectation of BM model of phenotypic evolution. Interestingly, we find that when the face is separated from the braincase, it also follows a BM process similar to the mandible. We interpret these findings to suggest that the rate of shape evolution in the facial module is being constrained and suppressed by its close proximity to the braincase, as well as a series of developmental mechanisms, including physical and molecular influences that create a strong pattern of covariation between the face and braincase regions (Hallgrímsson et al. 2009; Marcucio et al. 2011). This is strongly supported by previous studies on morphological integration between the face and the braincase across developmental series in dolichocephalic apteronotids (Evans et al. 2017b, 2017c).

The evolutionary rate and shape disparity of the braincase are likely constrained by its numerous functional interactions with other anatomical structures including the Weberian apparatus (a modification of the first four vertebrae which attach the swim bladder to the inner ear), numerous muscle attachments between facial and axial muscle groups, and housing the brain and many of the facial nerves (Fink and Fink 1981; Albert 2001). These numerous interactions may result in a high degree of functional integration which should, in-turn, impose powerful restrictions on the rate and trajectory of shape evolution in this module. It is possible that this pattern is conserved across all major teleost clades, as the braincase is burdened with many of the same multifunctional demands across this clade.

Perspectives on mosaic evolution across multifunctional structures

Multifunctional structures are prevalent throughout the natural world and present throughout several layers of biological organization. These structures are tasked with competing demands from separate functions that may exert opposing selective pressures across the structure. The evolutionary modularization of a multifunctional structure may serve to compartmentalize and localize selective forces to specific regions of the structure in an effort to relieve more globalized selective pressures. This modularization can then, in turn, facilitate mosaic patterns of

evolution as different regions of the structure begin to follow different evolutionary trajectories.

Evolutionary modularity is one of several potential solutions to dealing with competing selective demands across a structure (Linde-Medina et al. 2016). Evolutionary integration may also provide an alternative solution, allowing a structure to streamline responses to selective pressures if the angle between the primary direction of the trait covariances, and the varying directions of the selection vectors are sufficiently small (Goswami et al. 2014; Du et al. 2018). In this case, it is more likely that structures with fewer functions, or more similar functions, would utilize evolutionary integration as opposed to structures with more and diverse functions, which may instead utilize modularity.

As our ability to robustly and accurately sample morphologies continues to improve, and phylogenetic hypotheses for different groups become more prevalent and thoroughly sampled, we suspect it will become apparent that patterns of evolutionary mosaicism are broadly widespread across clades. While our ability to detect and quantify patterns of modularity and integration across structures has certainly improved (and will most likely continue to do so), the burden will then be on the investigators to identify and quantify the different functions that may be exerting selective pressures across them.

Acknowledgments

We would like to thank University of Washington Friday Harbor Labs and the #ScanAllFishes initiative for allowing us to scan our specimens free of charge. We would also like to acknowledge Javier Maldonado and Maxwell Bernt for providing rare apteronotid specimens for scanning. We would also like to acknowledge James Albert for his helpful advice.

Funding

VAT was supported by Fundação de Auxílio à Pesquisa do Estado de São Paulo (FAPESP #2018/20806-3). KME was supported by the CFANS Postdoctoral diversity fellowship.

Supplementary data

Supplementary data are available at *ICB* online.

References

Adams DC. 2016. Evaluating modularity in morphometric data: challenges with the RV coefficient and a new test measure. Methods Ecol Evol 7:565–72.

Albert JS. 2001. Species diversity and phylogenetic systematics of American knifefishes (Gymnotiformes, Teleostei). Division of Ichthyology, Museum of Zoology, University of Michigan.

Altschul SF, Gish W, Miller W, Myers EW, Lipman DJ. 1990. Basic local alignment search tool. J Mol Biol 215:403–10.

Benjamin M. 1990. The cranial cartilages of teleosts and their classification. J Anat 169:153–72.

Bennett D, Hettling H, Silvestro D, Zizka A, Bacon C, Faurby S, Vos R, Antonelli A. 2018. phylotaR: an automated pipeline for retrieving orthologous DNA sequences from GenBank in R. Life 8:20.

Bouckaert R, Heled J, Kühnert D, Vaughan T, Wu C-H, Xie D, Suchard MA, Rambaut A, Drummond AJ. 2014. BEAST 2: a software platform for Bayesian evolutionary analysis. PLoS Comput Biol 10:e1003537.

Brandon RN. 2005. Evolutionary modules: conceptual analyses and empirical hypotheses. In: Callebaut W, Rasskin-Gutman D, editors. Modularity: understanding the development and evolution of natural complex systems. Cambridge (MA): MIT Press. p. 51–60.

Buser TJ, Sidlauskas BL, Summers AP. 2017. 2D or not 2D? Testing the utility of 2D vs. 3D landmark data in geometric morphometrics of the sculpin subfamily Oligocottinae (Pisces; Cottoidea). Anat Rec 301:806–18.

Capella-Gutiérrez S, Silla-Martínez JM, Gabaldón T. 2009. trimAl: a tool for automated alignment trimming in large-scale phylogenetic analyses. Bioinformatics 25:1972–3.

Chapman L, Albert J, Galis F. 2008. Developmental plasticity, genetic differentiation, and hypoxia-induced trade-offs in an African cichlid fish. Open Evol J 2:75–88.

Cheverud JM. 1996. Developmental integration and the evolution of pleiotropy. Am Zool 36:44–50.

Clarke JA, Middleton KM. 2008. Mosaicism, modules, and the evolution of birds: results from a Bayesian approach to the study of morphological evolution using discrete character data. Syst Biol 57:185–201.

Collar DC, Wainwright PC, Alfaro ME, Revell LJ, Mehta RS. 2014. Biting disrupts integration to spur skull evolution in eels. Nat Commun 5:5505.

Drake AG, Klingenberg CP. 2010. Large-scale diversification of skull shape in domestic dogs: disparity and modularity. Am Nat 175:289–301.

Du TY, Tissandier SC, Larsson HC. 2018. Integration and modularity of teleostean pectoral fin shape and its role in the diversification of acanthomorph fishes. Evolution 73:401–11.

Eble GJ, Callebaut W, Rasskin-Gutman D. 2005. Morphological modularity and macroevolution: conceptual and empirical aspects. In: Modularity: understanding the development and evolution of natural complex systems. Cambridge, MA: MIT Press, p. 221–38.

Evans KM, Bernt MJ, Kolmann MA, Ford KL, Albert JS. 2018a. Why the long face? Static allometry in the sexually dimorphic phenotypes of Neotropical electric fishes. Zool J Linn Soc published online (https://doi.org/10.1093/zoolinnean/zly076).

Evans KM, Crampton WG, Albert JS. 2017a. Taxonomic revision of the deep channel electric fish genus *Sternarchella* (Teleostei: Gymnotiformes: Apteronotidae), with descriptions of two new species. Neotrop Ichthyol 15.

Evans KM, Savage AM, Albert JS. 2018b. Spinal abnormalities in a specimen of the Panamanian knifefish *Apteronotus rostratus* (Apteronotidae: Gymnotiformes) with comments on gymnotiform locomotion. Copeia 106:130–4.

Evans KM, Waltz B, Tagliacollo V, Chakrabarty P, Albert JS. 2017b. Why the short face? Developmental disintegration of the neurocranium drives convergent evolution in neotropical electric fishes. Ecol Evol 7:1783–801.

Evans KM, Waltz BT, Tagliacollo VA, Sidlauskas BL, Albert JS. 2017c. Fluctuations in evolutionary integration allow for big brains and disparate faces. Sci Rep 7:40431.

Federhen S. 2012. The NCBI taxonomy database. Nucleic Acids Res 40:D136–43.

Felice RN, Goswami A. 2017. Developmental origins of mosaic evolution in the avian cranium. Proc Natl Acad Sci U S A 115:555–60.

Felice RN, Randau M, Goswami A. 2018. A fly in a tube: macroevolutionary expectations for integrated phenotypes. Evolution 72:2580–94.

Felsenstein J. 1985. Phylogenies and the comparative method. Am Nat 125:1–15.

Fink SV, Fink WL. 1981. Interrelationships of the ostariophysan fishes (Teleostei). Zool J Linn Soc 72:297–353.

Goswami A. 2007. Cranial modularity and sequence heterochrony in mammals. Evol Dev 9:290–8.

Goswami A, Finarelli JA. 2016. EMMLi: a maximum likelihood approach to the analysis of modularity. Evolution 70:1622–37.

Goswami A, Polly PD. 2010. The influence of modularity on cranial morphological disparity in Carnivora and Primates (Mammalia). PLoS ONE 5:e9517.

Goswami A, Smaers J, Soligo C, Polly P. 2014. The macroevolutionary consequences of phenotypic integration: from development to deep time. Phil Trans R Soc B 369:20130254.

Hallgrímsson B, Jamniczky H, Young NM, Rolian C, Parsons TE, Boughner JC, Marcucio RS. 2009. Deciphering the palimpsest: studying the relationship between morphological integration and phenotypic covariation. Evol Biol 36:355–76.

Harmon LJ, Weir JT, Brock CD, Glor RE, Challenger W. 2008. GEIGER: investigating evolutionary radiations. Bioinformatics 24:129–31.

Hegrenes S. 2001. Diet-induced phenotypic plasticity of feeding morphology in the orangespotted sunfish, *Lepomis humilis*. Ecol Freshw Fish 10:35–42.

Helfman G, Collette BB, Facey DE, Bowen BW. 2009. The diversity of fishes: biology, evolution, and ecology. Hoboken, NJ: John Wiley & Sons.

Hill JJ, Puttick MN, Stubbs TL, Rayfield EJ, Donoghue PC. 2018. Evolution of jaw disparity in fishes. Palaeontology published online (doi:10.1111/pala.12371).

Hu Y, Albertson RC. 2017. Baby fish working out: an epigenetic source of adaptive variation in the cichlid jaw. Proc R Soc B 284:20171018.

Katoh K, Kuma K-I, Toh H, Miyata T. 2005. MAFFT version 5: improvement in accuracy of multiple sequence alignment. Nucleic Acids Res 33:511–8.

Keeffe R, Hilton EJ, De Souza MJFT, Fernandes CC. 2019. Cranial morphology and osteology of the sexually dimorphic electric fish, *Compsaraia samueli* Albert Crampton (Apteronotidae, Gymnotiformes), with comparisons to *C. compsa* (Mago-Leccia). Zootaxa 4555:101–12.

Kolmann MA, Huie JM, Evans K, Summers AP. 2018. Specialized specialists and the narrow niche fallacy: a tale of scale-feeding fishes. R Soc Open Sci 5:171581.

Küttner E, Parsons KJ, Easton AA, Skúlason S, Danzmann RG, Ferguson MM. 2014. Hidden genetic variation evolves with ecological specialization: the genetic basis of phenotypic plasticity in Arctic charr ecomorphs. Evol Dev 16:247–57.

Lanfear R, Frandsen PB, Wright AM, Senfeld T, Calcott B. 2016. PartitionFinder 2: new methods for selecting partitioned models of evolution for molecular and morphological phylogenetic analyses. Mol Biol Evol 34:772–3.

Langille RM, Hall BK. 1988. Role of the neural crest in development of the cartilaginous cranial and visceral skeleton of the medaka, *Oryzias latipes* (Teleostei). Anat Embryol 177:297–305.

Liem KF. 1993. Ecomorphology of the teleostean skull. Skull 3:422–52.

Linde-Medina M, Boughner JC, Santana SE, Diogo R. 2016. Are more diverse parts of the mammalian skull more labile? Ecol Evol 6:2318–24.

Mabee PM, Trendler TA. 1996. Development of the cranium and paired fins in *Betta splendens* (Teleostei: Percomorpha): intraspecific variation and interspecific comparisons. J Morphol 227:249–87.

Marcucio RS, Cordero DR, Hu D, Helms JA. 2005. Molecular interactions coordinating the development of the forebrain and face. Dev Biol 284:48–61.

Marcucio RS, Young NM, Hu D, Hallgrimsson B. 2011. Mechanisms that underlie co-variation of the brain and face. Genesis 49:177–89.

Motta PJ. 1988. Functional morphology of the feeding apparatus of ten species of Pacific butterflyfishes (Perciformes, Chaetodontidae): an ecomorphological approach. Environ Biol Fish 22:39–67.

Murrell DJ. 2018. A global envelope test to detect non-random bursts of trait evolution. Methods Ecol Evol published online (doi:10.1111/2041-210X.13006).

Neuhauss S, Solnica-Krezel L, Schier AF, Zwartkruis F, Stemple DL, Malicki J, Abdelilah S, Stainier D, Driever W. 1996. Mutations affecting craniofacial development in zebrafish. Development 123:357–67.

Parsons KJ, Son YH, Crespel A, Thambithurai D, Killen S, Harris MP, Albertson RC. 2018. Conserved but flexible modularity in the zebrafish skull: implications for craniofacial evolvability. Proc R Soc B 285:20172671.

Parsons KJ, Taylor AT, Powder KE, Albertson RC. 2014. Wnt signalling underlies the evolution of new phenotypes and craniofacial variability in Lake Malawi cichlids. Nat Commun 5:3629.

Piras P, Buscalioni AD, Teresi L, Raia P, Sansalone G, Kotsakis T, Cubo J. 2014. Morphological integration and functional modularity in the crocodilian skull. Integr Zool 9:498–516.

Price SA, Holzman R, Near TJ, Wainwright PC. 2011. Coral reefs promote the evolution of morphological diversity and ecological novelty in labrid fishes. Ecol Lett 14:462–9.

Rambaut A, Drummond A. 2003. Tracer: a program for analysing results from Bayesian MCMC programs such as BEAST & MrBayes. University of Edinburgh, UK.
Ricklefs RE. 2006. Time, species, and the generation of trait variance in clades. Syst Biol 55:151–9.
Sanderson MJ, Boss D, Chen D, Cranston KA, Wehe A. 2008. The PhyLoTA Browser: processing GenBank for molecular phylogenetics research. Syst Biol 57:335–46.
Sanger TJ, Mahler DL, Abzhanov A, Losos JB. 2012. Roles for modularity and constraint in the evolution of cranial diversity among *Anolis* lizards. Evolution 66:1525–42.
Stebbins G. 1983. Mosaic evolution: an integrating principle for the modern synthesis. Experientia 39:823–34.
Thompson JD, Plewniak F, Ripp R, Thierry J-C, Poch O. 2001. Towards a reliable objective function for multiple sequence alignments. J Mol Biol 314:937–51.
Trainor PA, Melton KR, Manzanares M. 2003. Origins and plasticity of neural crest cells and their roles in jaw and craniofacial evolution. Int J Dev Biol 47:541–53.
Vidal-García M, Keogh JS. 2017. Phylogenetic conservatism in skulls and evolutionary lability in limbs—morphological evolution across an ancient frog radiation is shaped by diet, locomotion and burrowing. BMC Evol Biol 17:165.
Vidal-García M, Bandara L, Keogh JS. 2018. ShapeRotator: an R tool for standardized rigid rotations of articulated three-dimensional structures with application for geometric morphometrics. Ecol Evol 8:4669–75.
Wagner GP. 1996. Homologues, natural kinds and the evolution of modularity. Am Zool 36:36–43.
Wagner GP, Altenberg L. 1996. Perspective: complex adaptations and the evolution of evolvability. Evolution 50:967–76.
Wainwright PC, Bellwood DR, Westneat MW, Grubich JR, Hoey AS. 2004. A functional morphospace for the skull of labrid fishes: patterns of diversity in a complex biomechanical system. Biol J Linn Soc 82:1–25.
Wainwright PC, Lauder GV, Osenberg CW, Mittelbach GG. 1991. The functional basis of intraspecific trophic diversification in sunfishes. In: The unity of evolutionary biology. Portland, OR: Dioscorides Press. Portland, OR: Dioscorides Press. p. 515–28.
Westneat MW. 2004. Evolution of levers and linkages in the feeding mechanisms of fishes. Integr Comp Biol 44:378–89.
Westneat MW. 2005. Skull biomechanics and suction feeding in fishes. Fish Physiol 23:29–75.
Wimberger PH. 1992. Plasticity of fish body shape. The effects of diet, development, family and age in two species of *Geophagus* (Pisces: Cichlidae). Biol J Linn Soc 45:197–218.
Winther RG. 2001. Varieties of modules: kinds, levels, origins, and behaviors. J Exp Zool 291:116–29.